Validating Photometric and Colorimetric Consistency of Physically-Based Image Synthesis

Jakob Bärz, Niklas Henrich, and Stefan Müller, University of Koblenz, Germany

Abstract

The purpose of physically-based image synthesis is to predict the natural appearance of a scenario by simulating the distribution of light using radiometric quantities. A set of spectral measurements on the film plane of the virtual camera is computed to generate a two-dimensional projection of the scene. To guarantee photometric and colorimetric consistency, the measured incident radiance distributions are reproduced exactly on the display device by reconstructing spectra with the same luminance and chromaticity. Although a significant number of predictive rendering systems have been presented in the past, there is still a lack of a comprehensive model incorporating local reflection, light transport, measurement, and reproduction. Furthermore, despite the fact that some of these frameworks have been validated in the last decades, trustworthy reproduction of color and luminance is a challenging field of research. The mathematical model to simulate and reproduce physically-based images while preserving photometric and colorimetric consistency is summarized. As a proof of concept, we integrated the model into a ray tracing system to generate photorealistic images. To validate our approach, a virtual scene and a real model of a well-defined box scenario were built and evaluated by photometric and colorimetric measurements. The scenario included a GretagMacbeth ColorChecker to allow an accurate verification of both luminance and chromaticity values. The illumination was simulated using spectral path tracing and radiometric quantities for the light source and the materials. The projected image was reproduced on a colorimetrically characterized LC device. Our results show that the 1976 CIELAB differences between the measurements of the ColorChecker patches in the real world scene and on the monitor displaying the reproduction of our simulation are well below the Just Noticeable Difference threshold.

Introduction

Today, considerable research is spent developing algorithms to approximate global illumination in real-time using modern GPU techniques. These approaches suit the needs of computer-generated imagery for films and video games perfectly. But in the context of product design, decision-makers rely on a trustworthy colorimetric and photometric appearance of the synthetic images. Even in the field of predictive physically-based rendering, validating the computed quantities is not yet common practice. Furthermore, while local reflection models and light transport algorithms are well-studied, measuring the incident radiance on the virtual image plane and reproducing these spectra on the display device still require extensive research.

In this work, we summarize a comprehensive mathematical model to simulate and reproduce truly predictive images. We have assembled the formulae for local reflection and light transport, derived a measurement equation capable of predicting radiometric quantities, and elaborated the reproduction of CIE XYZ tristimulus values with the same luminance and chromaticity on a characterized display device. To prove physical correctness, the model was integrated into a spectral path tracing system providing radiometric consistency for the input values and the lighting simulation. The post-processing step guarantees a photometrically and colorimetrically consistent reproduction on the display. We constructed a well-defined box scene containing a ColorChecker and modeled an exact virtual representation to simulate a ground truth image for a specified perspective. This synthetic image was verified by measuring the patches of the ColorChecker on the display device and comparing the results with the measurements of the patches in the real world setup.

The remainder of the paper is organized as follows: Section *Related Work* reviews the most important publications on physically-based rendering and validation as well as device characterization. In section *Approach*, we compile the mathematical background on local reflection, light transport, measurement, and reproduction of color on display devices. The validation scenario and measurement process is outlined in section *Evaluation*. Section *Results* outlines the important findings of our verification and section *Conclusion* summarizes and discusses this paper.

Related Work

Predictive Rendering Recursive Ray Tracing, the first algorithm to accurately simulate reflections, refractions and shadows was presented by Whitted [36] in 1979. Distributing the ray directions allows the computation of motion blur, depth of field, soft shadows, and glossy reflections, as proposed by Cook et al. [5] in 1984. With the introduction of the Rendering Equa-

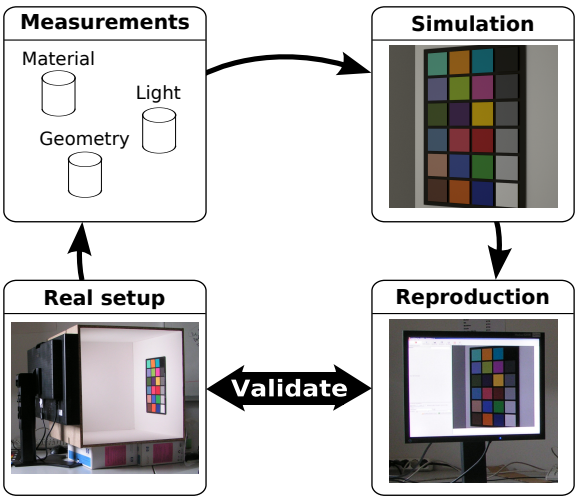

Figure 1. *Overview of our validation approach. The geometry and radiometric measurements of the physical scene serve as input for our spectral simulation. The generated image is reproduced on a characterized display. Measurements taken on the display are compared to the measurements taken in the box. (The photographs are included for illustrative purposes only.)*

tion and the Path Tracing algorithm by Kajiya [14] in 1986, it was possible to simulate global illumination including all light paths and to derive rendering methods from a common mathematical foundation. Important advancements include Bidirectional Path Tracing [16] [32], Metropolis Light Transport [32] and Photon Mapping [11] [12]. A comprehensive textbook on physically based rendering was presented by Pharr et al. [24] in 2004.

Ward [34] described a physically based rendering system using a ray tracing method to solve the rendering equation for complex materials, light sources and geometries by the name of Radiance in 1994. Addressing the demands of lighting design and architecture, the system was designed to be physically accurate, general in terms of handling the important lighting phenomena, and practical, i.e. reliable, usable and fast. A number of principal techniques are introduced to fulfill these goals.

In 1997, Greenberg et al. [10] presented a framework for realistic image synthesis. The goal was to support the development of physically based local reflection models (i.e. BRDFs) and light transport simulation algorithms as well as perceptually based visual display methods. They emphasized the importance of the fidelity of the physical simulation to guarantee predictive synthetic images. While the first two stages are validated by radiometric measurements, the third involves perceptual comparisons. Thus, the authors identified a number of difficulties like limited dynamic range, spatial resolution and color gamut of the display as well as the viewer's position, focus, state of adaption, and the complex relationship between spatial, temporal, and chromatic attributes of the scene.

Most important for our work, Greenberg et al. [10] validated the light transport measurements by acquiring two-dimensional CCD camera images of the real scene. After calibration, they obtained twelve-bit images at any wavelength using band pass filters. How these images were compared to either the simulated radiant energy on the virtual image plane or to the reproduced display output is not explained further.

Validation The first approach to verify synthetic images was to visually compare the rendering results with the respective real world scenario. In 1984, Goral et al. [9] showed the visual similarity between a radiosity rendering and a photograph of a cube with colored surfaces, the so called *Cornell Box*. Lacking quantitative results, this comparison validated the position of color bleeding effects but not the luminance or chromaticity values. Another subjective evaluation was carried out by McNamara et al. [20] in 2000 by performing an observer study with a real box environment and ten renderings of the setup with varying degree of quality. The cube was filled with objects colored in different levels of gray. The results led to the conclusion that some renderings offered the same perceptual quality as the real scene in terms of lightness of the materials. Recently, Meseth et al. [21] showed that measured bidirectional texture functions are superior to diffuse textures and the model of Phong [25] in a psychophysical user study.

In 1986, Meyer et al. [22] introduced radiometric measurements in addition to side-by-side comparisons to validate the lighting simulation and the color reproduction separately. Radiometric spot measurements were taken at 25 different locations in the real environment, consisting of a simple white cube containing an all-white box. These values were compared to the predicted quantities, calculated with the algorithm of Cohen and Greenberg [4]. The relative comparison between the real scene and the computed and reproduced values on a display device showed that the test persons were unable to distinguish the images.

Takagi et al. [29] validated their approach to realistic rendering by matching luminance and chromaticity spot measurements in a real car scene to the computed values in 1990. The work focused on a physically based rendering model, realistic materials, and a light model incorporating the sun, sky, weather, and time conditions. According to the authors, the measurements were almost equal to the simulated quantities. Furthermore, a number of approaches using a photometer to validate photorealistic renderings were made. Karner et al. [15] measured a grid of luminance values in a real office scene and compared these to simulated values from Radiance [34]. The reported root mean square error amounted to about 10% to 20%. Mardaljevic [18] presented a comprehensive validation of sky models rendered with Radiance [34] using photocells. Drago and Myszkowski [7] proposed the atrium at the University of Aizu as a new complex validation scene for predictive rendering and aquired 84 measurements using luxmeter probes. Comparing different material models, the lowest average simulation error of about 10% was obtained using measured BRDF data and Density Estimation Particle Tracing [33]. Another comprehensive validation study using luxmeter sensors was presented by Schregle et al. [28] in 2004. Their box scene consisted of both diffuse and specular materials. Using Photon Mapping [12] and Radiance [34], the average deviations of the simulated values were 2% and 1%, respectively.

Device Characterization A device characterization [2] aims to infer a transformation between the color space of the output device (usually device dependent RGB values) and a device independent color space (usually CIE XYZ). For our work, only the so-called *inverse* transformation, which predicts the device dependent RGB values necessary to reproduce a desired CIE XYZ tristimulus value, is of importance.

There are many characterization models available (a comprehensive overview is given in [31] or [27]). Our work relies on the research centered around the *piecewise linear interpolation assuming constant chromaticity coordinates* (PLCC) model [26, 8, 27] as this model is easy to invert analytically and requires only a few measurements. This model assumes that the primaries of the display are independent and that the chromaticity coordinates of the output of each channel are constant regardless of the digital input value. There are more complex models available, which account for variations in chromaticity [31, 6]. These models require significantly more measurements and are not invertible analytically [30]. Furthermore, there are models [3, 35] which account for channel interdependence (also called primary crosstalk) as well, but the inverse transformation is quite involved.

Approach

Physically-based rendering aims at synthesizing and displaying images on an output device to invoke the same color sensation in the mind of a human observer as the respective real-world scene. In order to simulate and reproduce images with the same luminance and chromaticity, a number of subtasks are obligatory. Therefore, we developed a comprehensive mathematical model. The first step involves taking a set of spectral measurements from a well-defined perspective on a two-dimensional film plane of a virtual camera. To accurately compute the spectral radiance distribution incident to the virtual film plane, a measurement equation is needed. As the overall goal is to simulate the distribution of light in a virtual scene, a concise mathematical

model to simulate the light transport including local reflections must be developed. When displaying the simulation, metamers of the radiance distribution incident on the virtual film plane are to be reproduced by the output device. Therefore, a display characterization model which accounts for the characteristics of the output device, is necessary. In the following, the important parts are described in more detail.

Measurement Equation The measurement equation [23] relates the output signal of an instrument for optical radiation measurement to the incident distribution of spectral radiance at the receiving aperture. In computer graphics, the sensing device is idealized to the virtual film of the simulated camera. The spatial and directional variance of the sensor is characterized by the responsivity function. This function accounts for the contribution of the measurements to the picture elements of the synthetic image.

Let $\mathscr{M}$ be the union of the surfaces in $\mathbb{R}^3$ modeling the scene geometry and $\mathscr{S}^2$ the set of all possible unit-length vectors $\omega \in \mathbb{R}^3$. The radiant flux incident to pth picture element can be measured by:

$$\Phi_p(x,\omega) = \int_{\mathscr{M}} \int_{\mathscr{S}^2} W_p(x,\omega)\, L_i(x,\omega)\, |cos\theta_i|\, d\omega\, dx \qquad (1)$$

The responsivity $W_p(x,\omega)$ is the product of the filter function $f_p(x)$ around the pth picture element and a delta function accounting for the optical path ω_x within the receiving aperture for each individual measurement. Since we are not aiming at a simulation of a real camera system, we model the virtual film as a bare plane receiver-detector with uniform isotropic response and the optical lens system as a lossless, isotropic, iso-refractive-index medium:

$$W_p(x,\omega) = f_p(x)\, \delta(\omega_x - \omega) \qquad (2)$$

Using a normalized box filter function

$$\begin{aligned} f_p(x) &= \begin{cases} A_p^{-1} & \text{if } x \in A_p \subset \mathscr{M} \\ 0 & \text{else} \end{cases} \\ \textstyle\int_{\mathscr{M}} f_p(x)\, dx &= 1 \end{aligned}$$

and the properties of the delta function

$$\begin{aligned} \textstyle\int_{\mathscr{S}^2} \delta(\omega_x - \omega) g(\omega)\, d\omega &= g(\omega_x) \\ \textstyle\int_{\mathscr{S}^2} \delta(\omega_x - \omega)\, d\omega &= 1 \\ [\delta(\omega_x - \omega)] &= sr^{-1} \end{aligned}$$

yields

$$L_p(x,\omega) = \frac{1}{A_p} \int_{A_p} L_i(x,\omega_x)\, |cos\theta_i|\, dx \qquad (3)$$

Light Transport Equation In order to compute the incident radiance $L_i(x,\omega_x)$ on the film, it is convenient to express this quantity in terms of exitant radiance using the geometrical invariance in a passive, lossless, uniform, and isotropic medium:

$$L_i(x,\omega_x) = L_o(x_{\mathscr{M}}(x,\omega_x), -\omega_x) \qquad (4)$$

We define $x_{\mathscr{M}}(x,\omega_x)$ as the ray-casting operator [32], returning the first visible point $p \in \mathscr{M}$ from x in direction ω_x.

For physically-based image synthesis, it is adequate to assume incoherent radiation obeying the physical laws of geometrical ray optics. Thus, the light transport equation formulates the equilibrium radiance distribution mathematically. For a given point of intersection p and exitant direction $v = -\omega_x$ the exitant radiance is given by:

$$L_o(p,v) = L_e(p,v) + \int_{\mathscr{S}^2} f(p,v,\omega)\, L_i(p,\omega)\, |cos\theta_i|\, d\omega \qquad (5)$$

The Light Transport Equation is computed by ray tracing algorithms using Monte-Carlo methods. In photorealistic computer graphics, it is conventional to simulate ground-truth results by Path Tracing [14]. To decrease noise, typical variance reduction strategies like splitting and multiple importance sampling are applied [24]. Eq.5 is the sum of emitted, direct, and indirect illumination. As a part of the scene description, the emitted radiance $L_e(p,v)$ is directly evaluated as a function of position and direction. The direct radiance $L_d(p,v)$ is computed effectively by explicitly sampling the light sources. Introducing the geometrical term

$$G(p,p') = V(p,p') \frac{|cos\theta||cos\theta'|}{||p-p'||^2} \qquad (6)$$

where V is a binary visibility function and expressing the hemispherical integral as an integral over all the surfaces of the light sources in the scene, we write:

$$L_d(p,v) = \int_{\mathscr{M}} f(p,v,\omega)\, L_e(p',-\omega)\, G(p,p')\, dp' \qquad (7)$$

As is customary, indirect radiance $L_{id}(p,v)$ is solved by importance sampling of the BRDF.

Radiometric Data To solve the Light Transport Equation (see Eq.5) while preserving radiometric consistency, radiometric parameters for all the light sources and spectral distributed BRDFs for all materials in the virtual scene are obligatory (how these values are acquired will be explained in the next section). After the simulation, the resulting radiance distributions on the virtual film plane are converted to photometric values by applying the CIE color-matching functions $\bar{x}$, $\bar{y}$ and $\bar{z}$[37]. It is necessary to use the same color-matching functions as the physical measurement device for the validation (in our case the CIE Standard 1931 observer functions). The following equation transforms a spectral radiance distribution $L(\lambda)$ into the device-independent color space XYZ:

$$C = \int_{\lambda_1}^{\lambda_2} k \cdot L(\lambda) \cdot \bar{c}(\lambda)\, d\lambda \qquad (8)$$

with $C \in \{X,Y,Z\}$ and $c \in \{x,y,z\}$. In order to properly convert between radiometric and photometric units, the constant k is set to $683 \frac{lm}{W}$.

Device Characterization The LC display is characterized by an inverse *piecewise linear interpolation assuming constant chromaticity coordinates* (PLCC) model [27]. This model assumes that the device's primaries are independent and thus additivity is given. It further implies that the chromaticity of the primaries is constant. While this assumption holds true for most CRT devices, LC devices usually suffer from a lack thereof [8]. Jimnez del Barco et al. [13] showed that measuring the black level of LC devices and taking this value into account produces chromaticity constancy for most LC devices.

The following transformation predicts the device dependent RGB values (normalized to 1) needed to produce the same color sensation to a human observer as the desired CIE XYZ value:

$$\begin{bmatrix} R' \\ G' \\ B' \end{bmatrix} = \begin{bmatrix} X_R - X_0 & X_G - X_0 & X_B - X_0 \\ Y_R - Y_0 & Y_G - Y_0 & Y_B - Y_0 \\ Z_R - Z_0 & Z_G - Z_0 & Z_B - Z_0 \end{bmatrix}^{-1} \begin{bmatrix} X - X_0 \\ Y - Y_0 \\ Z - Z_0 \end{bmatrix} \quad (9)$$

$\begin{bmatrix} X_K & Y_K & Z_K \end{bmatrix}^T$, $K \in \{R,G,B\}$ denote the CIE XYZ values measured when the red, green, and blue primaries are set to their maximum intensity and $\begin{bmatrix} X_0 & Y_0 & Z_0 \end{bmatrix}^T$ when they are set to their minimum intensity. If the measurement device is not capable of measuring the black point, methods from [1] can be used to estimate a reasonable value.

After the linear transformation from CIE XYZ to device-dependent RGB values by means of the primary transform matrix, a non-linear transformation has to be applied to the RGB values prior to sending them to the display. A Tone Reproduction Curve (TRC), corresponding to a power function with the reciprocal of the display's gamma value as the exponent, is applied per channel. We assume that the TRC is the same for each channel C, $C \in \{R,G,B\}$: $C = C'^{\frac{1}{\gamma}}$.

Evaluation

To validate the photometric and colorimetric consistency of both our lighting simulation and color reproduction, we conducted a direct comparison between a real world scene and a simulation of a virtual representation of the same scene, displayed on an LC display (see Fig.1). We constructed a well-defined real world scenario and modeled an exact virtual representation of the geometry. A ground-truth simulation was computed using our spectral path tracing system and radiometrically measured input parameters for the materials and the light source. The simulated two-dimensional projection was displayed on the colorimetrically characterized display device (NEC SpectraView 2690). A luminance and color meter (Konica Minolta CS-100A) was used to generate a set of spot measurements for comparison.

Scenario The scenario consisted of a cubical box, measuring $0.5m$ in all three dimensions. The front side was left open for the observer or measurement device. In the center of the left side, a square hole with $0.3m$ edge length was spared for a calibrated NEC SpectraView 2690 as the light source. On the right, opposing the illuminant, a GretagMacbeth ColorChecker chart was placed. The remainder of the interior of the box was wallpapered with a diffuse white Canson Mi-Teintes paper.

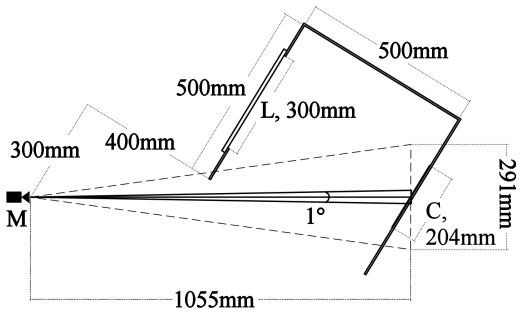

Figure 2. *Outline of the measurement setup in the real box. Horizontal cut through the center of the box. The cube has a size of* $(500mm)^3$*. The measurement device* ***M*** *with an acceptance angle of* 1° *is placed* $300mm$ *before and* $400mm$ *left of the box in a distance of* $1055mm$ *to the ColorChecker* ***C*** *with a width of* $204mm$*. The square light source* ***L*** *with the dimensions* $(300mm)^2$ *is opposite the ColorChecker. The dashed lines show the field of view of the virtual camera with the same optical center as the measurement device.*

Measurements and Simulation The spectral distributed radiance of the light source and the spectral distributed reflectance of the materials were measured with an X-Rite i1-pro spectroradiometer. The $0.3m \times 0.3m$ area light source was subdivided into 25 tiles. Each tile was measured separately multiple times and then averaged. The directional distribution was accounted for by measuring the fall-off for nine different angles in both horizontal and vertical direction. A light distribution curve was fitted to the acquired data. An exact virtual representation was modeled of this box. The light distribution was simulated with path tracing using our spectral ray tracing framework (see section *Approach*).

Reproduction The two-dimensional set of spectral measurements on the virtual film plane was reproduced on the display device using the model described in paragraph *Device Characterization*. After a warm-up phase, the display device was calibrated with an X-Rite i1-pro spectroradiometer. The maximum luminance value of the display was adjusted so that all luminance values of the color checker patches were within the dynamic range of the output device. Therefore no Tone Mapping operator had to be applied to the output image which could have falsified the results. The white point of the display was set to its native white point and the gamma value to 2.2. The columns of the primary transform matrix (see Eq.9) as well as the black point were measured several times at the center of the screen. The averages of the respective measurements were used.

Validation To validate our mathematical model, the path tracing simulation, and the color reproduction, we conducted a number of measurements using a color meter. Firstly, we measured the luminance and chromaticity values at the center of each of the 24 patches of the ColorChecker in the real box scene from a fixed view point (see Fig. 2). A distance of $1055mm$ between the optical center of the measurement device and the center of the ColorChecker ensured compliance with the focusing distance while maintaining homogeneous spot measurements.

Secondly, the simulated image of the virtual scene was reproduced on the display. Again, the color meter was placed at a distance of $1055mm$ from the center of the ColorChecker, displayed on the output device (see Fig. 3). The position and viewing direction of the virtual camera in the modeled scene was exactly the same as the position and direction of the measurement device in the real setup. A resolution of 1014^2 was chosen for the synthetic image to ensure that the displayed ColorChecker has the same height of $291mm$ as the real one: $1014 \cdot 0.287mm\,(dot\,pitch) \approx 291mm$. Thus, the projected area of each of the patches within the acceptance angle of the measurement device was identical for both real world and display setup. Finally, all measurements were converted to the CIELAB color space. The differences between the various measurements were compared by means of the 1976 CIELAB color difference equation.

Results

First, we will show the evaluation results of the whole process chain: from the measurements in the real scene to the simulation and eventually to the reproduction on the display.We compared the CIE XYZ values of the 24 patches of the GretagMac-

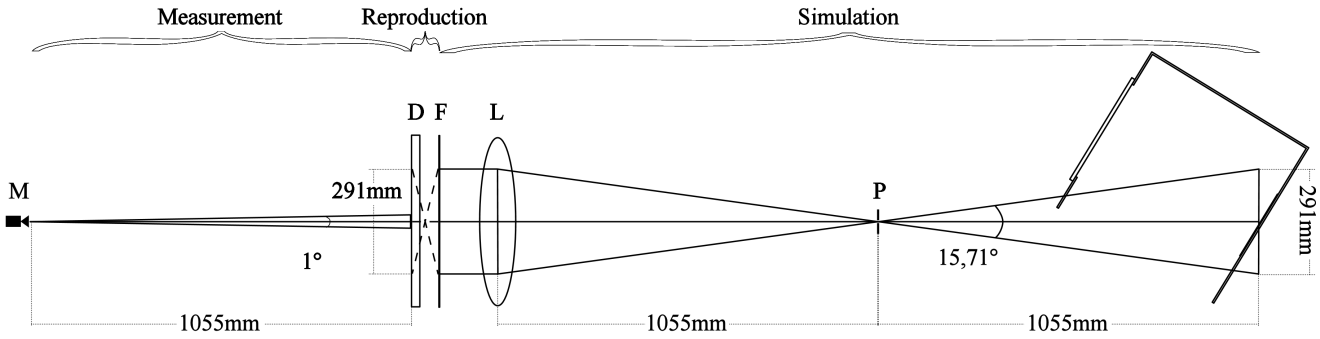

Figure 3. *Outline of the measurement setup on the display device. Horizontal cut through the center of the display image. From right to left, the simulation, the reproduction, and the measurement are visualized. The virtual pinhole camera* ***P*** *of the simulation is defined to have the same position and viewing direction in the virtual scene as the measurement device in the real scene. A field of view of* $15,71°$ *and an aspect ratio of* $1:1$ *guarantees the full visibility of the ColorChecker with a total height of* $291mm$*. The idealized lens* ***L*** *ensures the parallelization and the orthogonal incidence of the viewing rays to the virtual film plane* ***F****. The synthetic image is reflected at its center and reproduced on the display device* ***D****. An image resolution of* 1014×1014 $dots$ *guarantees, that the displayed image has exactly the same size and perspective as the respective out-take of the real scene from the measurement device's point of view.*

beth ColorChecker [19] measured in the box with the measurements of the simulation, reproduced on an LC display. As a difference measure, we used the 1976 CIELAB color difference formula [37] and the white point of the display as reference white for all conversions. All 24 CIE XYZ values were within the gamut of the display device.

Fig.4 shows that 21 out of 24 patches could be reproduced accurately. The ΔE^*_{ab} differences of these patches lie beneath the Just Notable Difference of approximately 2.3 [17]. To analyze the differences in chromaticity between the measured patches and the simulated and reproduced patches, they are projected onto the $a*b*$ plane. As visualized on the left in Fig.5, the differences are minor except for the two strong outliers also identified in Fig.4. Taking luminance into consideration, it is evident that our approach was successful in reproducing nearly all measured samples (again, except for the two strong outliers) with great accuracy (see right hand side of Fig.5). Comparing the projection onto the $a*b*$ and the $L*a*$ plane, leeds to the conclusion that there is no clear tendency whether the small differences between the measured and the simulated and reproduced samples are mainly due to differences in chromaticity or luminance.

We will now look at how well the simulation was able to reproduce the real conditions in the box in more detail. Fig.6 compares the CIE XYZ values measured in the box with the result of the simulation. It is apparent that nearly all patches could be simulated properly. Only two patches (13 and 15) lie well above the JND, while two patches lie just around the threshold. Also, it can be concluded from Fig.6 that the model used for the device characterization was sufficient in reliably reproducing the values of the simulation. After displaying the final image, with the exception of one sample (18), all samples below the JND after the simulation are also below the JND after the reproduction on the output device. Furthermore, two samples just around the JND were now below the threshold. This could have been caused in case the shift in chromaticity and luminance induced by the output happened to be in the direction of the measured value.

Conclusion

In conclusion, we presented the complete mathematical model to simulate truly predictive photorealistic images. The model includes the local reflection model, the light transport formula and a measurement equation, capable of computing accurate radiometric values for the synthetic image. Furthermore, we showed the necessary calculations to reproduce these spec-

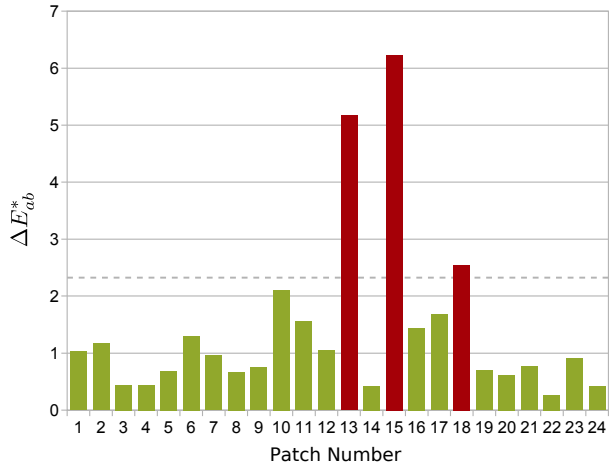

Figure 4. *Differences in units of* ΔE^*_{ab} *between the measurements of the 24 color checker patches taken in the box and on the LC device.*

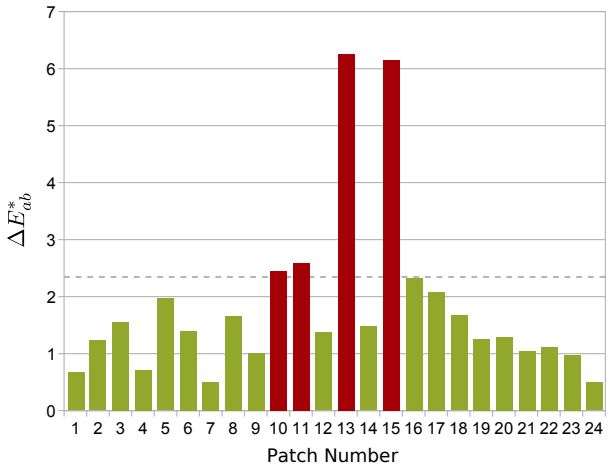

Figure 6. *Differences in units of* ΔE^*_{ab} *between the measurements of the 24 color checker patches taken in the box and the result of the simulation.*

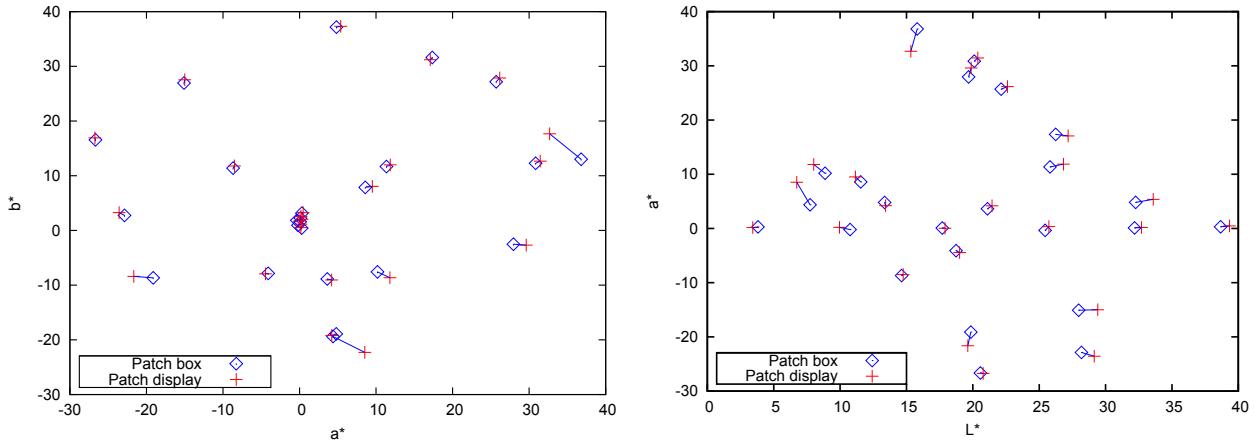

Figure 5. *The measurements of the 24 color checker patches taken in the box (Patch box) and after the lighting simulation and reproduction on the LC device (Patch display) projected onto the $a*b*$ plane (left) and the $L*a*$ plane (right) in the CIELAB color space.*

tral radiance distributions on a characterized display device while maintaining photometric and colorimetric consistency. The model was integrated into a spectral path tracing system to verify the simulation results. We constructed a well-defined box scene including a GretagMacbeth ColorChecker and a controllable illuminant to accurately validate both luminance and chromaticity values. A crucial point for all photorealistic image synthesis systems is the need for accurately measured materials, especially if the simulation is done radiometrically. This is especially true for the light sources, as the exact spectral radiance distribution and light distribution curve must be known for the validation. As it is very difficult to acquire light sources with this information, we overcame this problem by using a characterized LC device of which we were able to infer this information from.

Using the measured light source and materials as input values, we computed a ground-truth path tracing simulation using spectral quantities in all stages of the algorithm. The computed spectral radiance incident to the virtual film plane was converted to CIE XYZ tristimulus values with the same luminance and chromaticity. Both the simulated and the reproduced quantities were validated by spot measurements using a color meter. We measured the center of all 24 ColorChecker patches in the real box and on the LCD displaying the reproduced synthetic image. The color difference in CIELAB color space between the display measurements and the real world measurements were calculated. The results showed that the complete system including measurements, simulation, and display characterization was able to compute 21 of the 24 patches of the ColorChecker with an error below the Just Noticeable Difference threshold.

As far as the device characterization is concerned, the chosen approach has been successful in reproducing the simulated values. It can be concluded that an inverse *piecewise linear interpolation assuming constant chromaticity coordinates* (PLCC) model with black correction was a characterization model which accounted for most of the significant characteristics of an LC display device. It enabled us to reproduce the values of the simulation on the LC device with sufficient accuracy to be used for the measurements in our proposed validation approach.

References

[1] Roy S. Berns, Scot R. Fernandez, and Lawrence Taplin. Estimating black-level emissions of computer-controlled displays. *Color Research & Application*, 28(5):379–383, 2003.

[2] D.H. Brainard, D.G. Pelli, and T. Robson. Display characterization. encyclopedia of imaging science and technology, 2002.

[3] Yu-Kuo Cheng and Han-PingD. Shieh. Colorimetric characterization of high dynamic range liquid crystal displays and its application. *J. Display Technol.*, 5(1):40–45, 2009.

[4] Michael F. Cohen and Donald P. Greenberg. The hemi-cube: a radiosity solution for complex environments. In *SIGGRAPH '85: Proceedings of the 12th annual conference on Computer graphics and interactive techniques*, pages 31–40, New York, NY, USA, 1985. ACM.

[5] Robert L. Cook, Thomas Porter, and Loren Carpenter. Distributed ray tracing. *SIGGRAPH Comput. Graph.*, 18(3):137–145, 1984.

[6] Ellen A. Day, Lawrence Taplin, and Roy S. Berns. Colorimetric characterization of a computer-controlled liquid crystal display. *Color Research & Application*, 29(5):365–373, 2004.

[7] Frédéric Drago and Karol Myszkowski. Validation proposal for global illumination and rendering techniques. *Computers & Graphics*, 25(3):511–518, 2001.

[8] Mark Fairchild, Mark D. Fairchild, and David R. Wyble. Colorimetric characterization of the apple studio display (flat panel lcd). In *LCD), Munsell Color Science Laboratory Technical Report*, page http://www.cis.rit.e, 1998.

[9] Cindy M. Goral, Kenneth E. Torrance, Donald P. Greenberg, and Bennett Battaile. Modeling the interaction of light between diffuse surfaces. *SIGGRAPH Comput. Graph.*, 18(3):213–222, 1984.

[10] Donald P. Greenberg, Kenneth E. Torrance, Peter Shirley, James Arvo, Eric Lafortune, James A. Ferwerda, Bruce Walter, Ben Trumbore, Sumanta Pattanaik, and Sing-Choong Foo. A framework for realistic image synthesis. In *SIGGRAPH '97: Proceedings of the 24th annual conference on Computer graphics and interactive techniques*, pages 477–494, New York, NY, USA, 1997. ACM Press/Addison-Wesley Publishing Co.

[11] Henrik Wann Jensen. *Global Illumination - using Bidirectional Monte Carlo Ray Tracing*. PhD thesis, Dept. of Graphical Communication, Technical University of Denmark, 1993.

[12] Henrik Wann Jensen. *Realistic image synthesis using photon mapping*. A. K. Peters, Ltd., Natick, MA, USA, 2001.

[13] L. Del JimnezBarco, J. A. Daz, J. R. Jimnez, and M. Rubio. Considerations on the calibration of color displays assuming constant channel chromaticity. *Color Research & Application*, 20(6):377–387, 1995.

[14] James T. Kajiya. The rendering equation. *SIGGRAPH Comput. Graph.*, 20(4):143–150, 1986.

[15] Konrad F. Karner and Manfred Prantl. A concept for evaluating the accuracy of computer-generated images. In *Proceedings of the Twelfth Spring Conference on Computer Graphics (SCCG' 96)*, Comenius University, Bratslavia, Slovakia, June 1996.

[16] Eric P. Lafortune and Yves D. Willems. Bi-directional path tracing. In H. P. Santo, editor, *Proceedings of Third International Conference on Computational Graphics and Visualization Techniques (Compugraphics '93)*, pages 145–153, Alvor, Portugal, 1993.

[17] M. Mahy, L. Van Eycken, and A. Oosterlinck. Evaluation of uniform color spaces developed after the adoption of cielab and cieluv. *Color Res. Appl.*, 19:105–121, 1994.

[18] J Mardaljevic. *Daylight Simulation: Validation, Sky Models and Daylight Coefficients*. PhD thesis, De Montfort University, Institute of Energy and Sustainable Development, Leicester, 1999.

[19] Calvin S. McCamy, H. Marcus, and J. G. Davidson. A color-rendition chart. *J. Appl. Photogr. Eng.*, 2(3):95–99, Summer 1976.

[20] Ann McNamara, Alan Chalmers, Tom Troscianko, and Iain Gilchrist. Comparing real & synthetic scenes using human judgements of lightness. In *Proceedings of the Eurographics Workshop on Rendering Techniques 2000*, pages 207–218, London, UK, 2000. Springer-Verlag.

[21] Jan Meseth, Gero Müller, Reinhard Klein, Florian Röder, and M. Arnold. Verification of rendering quality from measured btfs. In *The 3rd Symposium on Applied Perception in Graphics and Visualization*, July 2006.

[22] Gary W. Meyer, Holly E. Rushmeier, Michael F. Cohen, Donald P. Greenberg, and Kenneth E. Torrance. An experimental evaluation of computer graphics imagery. *ACM Trans. Graph.*, 5(1):30–50, 1986.

[23] F. E. (ed.) Nicodemus. *Self-Study Manual on Optical Radiation Measurements: Part I-Concepts*. National Bureau of Standards (US), 1978.

[24] Matt Pharr and Greg Humphreys. *Physically Based Rendering : From Theory to Implementation*. Morgan Kaufmann, August 2004.

[25] Bui Tuong Phong. Illumination for computer generated pictures. *Commun. ACM*, 18(6):311–317, 1975.

[26] David L. Post and Christopher S. Calhoun. An evaluation of methods for producing desired colors on crt monitors. *Color Research & Application*, 14(4):172–186, 1989.

[27] David L. Post and Christopher S. Calhoun. Further evaluation of methods for producing desired colors on crt monitors. *Color Research & Application*, 25(2):90–104, 2000.

[28] Roland Schregle and Jan Wienold. Physical validation of global illumination methods: Measurement and error analysis. *Comput. Graph. Forum*, 23(4):761–781, 2004.

[29] Atsushi Takagi, Hitoshi Takaoka, Tetsuya Oshima, and Yoshinori Ogata. Accurate rendering technique based on colorimetric conception. *SIGGRAPH Comput. Graph.*, 24(4):263–272, 1990.

[30] J.-B. Thomas, P. Colantoni, J. Y. Hardeberg, I. Foucherot, and P. Gouton. An inverse display color characterization model based on an optimized geometrical structure. In *Society of Photo-Optical Instrumentation Engineers (SPIE) Conference Series*, volume 6807 of *Society of Photo-Optical Instrumentation Engineers (SPIE) Conference Series*, January 2008.

[31] Jean-Baptiste Thomas, Jon Y. Hardeberg, Irne Foucherot, and Pierre Gouton. The plvc display color characterization model revisited. *Color Research & Application*, 33(6):449–460, 2008.

[32] Eric Veach. *Robust monte carlo methods for light transport simulation*. PhD thesis, Stanford University, 1998.

[33] Valdimir Volevich, Karol Myszkowski, Andrei Khodulev, and Edward A. Kopylov. Using the visual differences predictor to improve performance of progressive global illumination computation. *ACM Trans. Graph.*, 19(2):122–161, 2000.

[34] Gregory J. Ward. The radiance lighting simulation and rendering system. In *SIGGRAPH '94: Proceedings of the 21st annual conference on Computer graphics and interactive techniques*, pages 459–472, New York, NY, USA, 1994. ACM.

[35] Senfar Wen and Royce Wu. Two-primary crosstalk model for characterizing liquid crystal displays. *Color Research & Application*, 31(2):102–108, 2006.

[36] Turner Whitted. An improved illumination model for shaded display. *SIGGRAPH Comput. Graph.*, 13(2):14, 1979.

[37] Günther Wyszecki and W. S. Stiles. *Color Science: Concepts and Methods, Quantitative Data and Formulae (Wiley Series in Pure and Applied Optics)*. Wiley-Interscience, 2 edition, August 2000.

